Thermal and magnetic field-induced martensite-austenite transition in $Ni_{50.3}Mn_{35.3}Sn_{14.4}$ ribbons

B. Hernando,[a] J. L. Sánchez Llamazares, and J. D. Santos
Departamento de Física, Facultad de Ciencias, Universidad de Oviedo, Calvo Sotelo s/n, 33007 Oviedo, Spain

Ll. Escoda and J. J. Suñol
Universidad de Girona, Campus de Montilivi, edifici PII, Lluís Santaló s/n, 17003 Girona, Spain

R. Varga
Institute of Physics, Faculty of Science, UPJS, Park Angelinum 9, 04154 Kosice, Slovakia

D. Baldomir and D. Serantes
Departamento de Física Aplicada, Facultad de Física, Universidad de Santiago de Compostela, Campus Sur s/n, 15782 Santiago de Compostela, Spain

(Received 14 November 2007; accepted 26 December 2007; published online 29 January 2008)

Thermal and field-induced martensite-austenite transition was studied in melt spun $Ni_{50.3}Mn_{35.3}Sn_{14.4}$ ribbons. Its distinct highly ordered columnarlike microstructure normal to ribbon plane allows the direct observation of critical fields at which field-induced and highly hysteretic reverse transformation starts ($H=17$ kOe at 240 K), and easy magnetization direction for austenite and martensite phases with respect to the rolling direction. Single phase $L2_1$ bcc austenite with T_C of 313 K transforms into a $7M$ orthorhombic martensite with thermal hysteresis of 21 K and transformation temperatures of $M_S=226$ K, $M_f=218$ K, $A_S=237$ K, and $A_f=244$ K. © *2008 American Institute of Physics*. [DOI: 10.1063/1.2838356]

Since martensitic transformation from cubic $L2_1$-type crystal structure to orthorhombic four-layered martensite (4O) was observed in Heusler alloys of the ternary system $Ni_{50}Mn_{50-x}Sn_x$,[1] important attention has been devoted to investigate structural transformations, magnetoelastic and magnetocaloric properties in these Ga-free ferromagnetic shape memory alloys.[2–11] The studies concluded that these materials are prospective for the development of magnetically driven actuators and working substances for magnetic refrigeration. The occurrence of ferromagnetism in both phases has been only found in the narrow composition range of $13 \leqslant x \leqslant 15$,[2] and the different magnetization values between martensite and austenite phases leads to a large magnetocaloric effect around the martensitic transition.[7,9] Their crystal structures, as well as the characteristic temperatures of its mutual reversible transformation (the starting and finish martensitic and austenitic temperatures, M_S, M_f, A_S, and A_f, respectively), are very sensitive to small variations in the valence electron concentration per atom e/a,[2,3] and consequently to chemical composition and also depends on the magnetic applied field. The magnetic field can also induce a reverse structural transformation as has been unambiguously demonstrated studying field dependence of x-ray diffraction (XRD) profiles in bulk polycrystalline $Ni_{50}Mn_{36}Sn_{14}$ alloys,[6] where a field higher than 50 kOe was required to induce around A_S a complete phase transition.

Rapid quenching by melt spinning offers two potential advantages for the fabrication of these magnetic shape memory alloys: the avoiding, or reduction, of the annealing to reach a homogeneous single phase alloy, and the synthesis of highly textured polycrystalline ribbons. In addition, ribbon shape can be also more appropriate for use in practical devices. Recently, we reported that it was an effective single-step production process for obtaining $Ni_{50}Mn_{37}Sn_{13}$ ribbons with homogenous chemical composition and strongly ordered microstructure.[12] In this letter, we report on the thermal and magnetic field-induced martensite-austenite transformation, microstructural, and magnetic properties of $Ni_{50.3}Mn_{35.3}Sn_{14.4}$ alloy ribbons.

Ribbon flakes of width about 1.5–2.0 mm and length of 6–7 mm were produced by melt spinning in argon atmosphere at a wheel linear speed of 48 ms^{-1} starting from arc melted alloys prepared from highly pure elements (>99.9%). Samples were annealed in high vacuum for 2 h at 1073 K. Annealing was followed by water quenching. Microstructure and elemental compositions were examined by using a scanning electron microscope (SEM) equipped with an x-ray energy dispersive spectroscopy (EDS) system. SEM examinations in backscattering emission mode revealed that chemical elements tend to distribute homogeneously in the alloy. EDS analyses performed on the cross section and both ribbon surfaces of different flakes gave the average composition $Ni_{50.3}Mn_{35.3}Sn_{14.4}$. XRD analyses were performed using Cu $K\alpha$ radiation in a low temperature diffractometer. Zero-field cooling (ZFC), field cooling (FC), and field heating (FH) thermomagnetic curves were recorded from 4.2 to 350 K for applied fields of 50 and 50 kOe, along the ribbon axis (i.e., rolling direction), with a heating or cooling rate of 2 K/min, using a physical properties measuring system platform with a vibrating-sample magnetometer module. Curie point T_C was inferred from the minimum in the dM/dT versus T curve. Hysteresis loops were measured up to 10 kOe using a superconducting quantum interference device.

SEM micrographs of the fracture morphology and free surface of ribbons are shown in Fig. 1, where a highly ordered columnar microstructure is observed. Individual col-

[a]Author to whom correspondence should be addressed. Electronic mail: grande@uniovi.es.

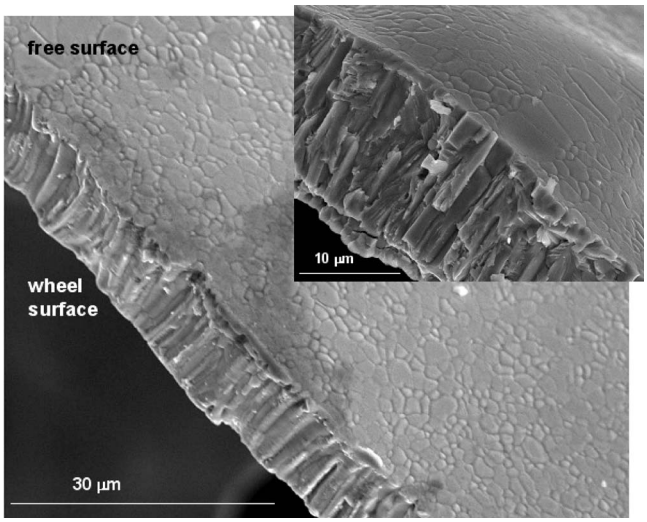

FIG. 1. SEM micrograph showing the fractured cross section and free surface of $Ni_{50.3}Mn_{35.3}Sn_{14.4}$ ribbons. Inset: higher magnification micrograph.

umns grow perpendicular to the ribbons plane from a thin layer of small equiaxed crystallized grains at the surface in contact with the wheel. They run through the entire ribbon thickness around 7–10 μm. Ribbons are brittle and easy to cleave in such direction.

$M(T)$ curves recorded at 50 Oe in ZFC, FC, and FH modes with those recorded at 50 kOe on heating and cooling are compared in Fig. 2. The inset shows the corresponding dM/dT versus T curve at low field. In the ZFC curve, $M(T)$ is zero with the increasing temperature up to 100 K, afterward a quasilinear monotonic increase starts. At 236 K, an abrupt and sharp increase in the magnetization suggests the occurrence of martensite-austenite transformation. X-ray diffraction patterns were obtained at a temperature below and above the transformation for phase identification (Fig. 3). At 270 K, the sample is a single phase austenite with cubic bcc $L2_1$ crystal structure and lattice parameter $a=0.5977$ nm, while the obtained one at 150 K was indexed on the basis of a modulated 7M orthorhombic martensite showing lattice parameters $a=0.6162$ nm, $b=0.6048$ nm, and $c=0.5633$ nm. Traces of secondary or spurious phases were not detected. Structures of both phases coincide with the found ones in as-spun ribbons,[12] but the modulation of the orthorhombic

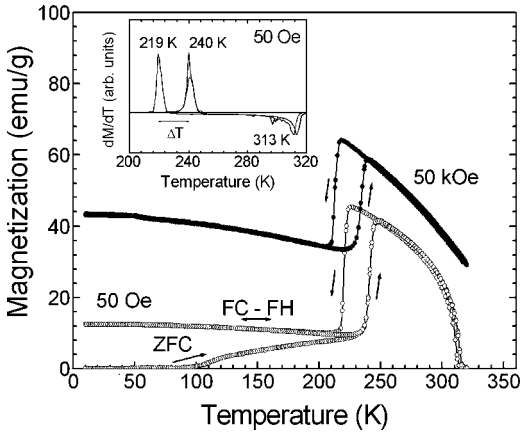

FIG. 2. Temperature dependence of the magnetization measured at $H=50$ Oe, and $H=50$ kOe, for $Ni_{50.3}Mn_{35.3}Sn_{14.4}$ ribbons. The arrows indicate whether the curve corresponds to heating or cooling regimen. Inset: dM/dT curve at 50 Oe, the horizontal double arrow indicates the thermal hysteresis of the structural transformation.

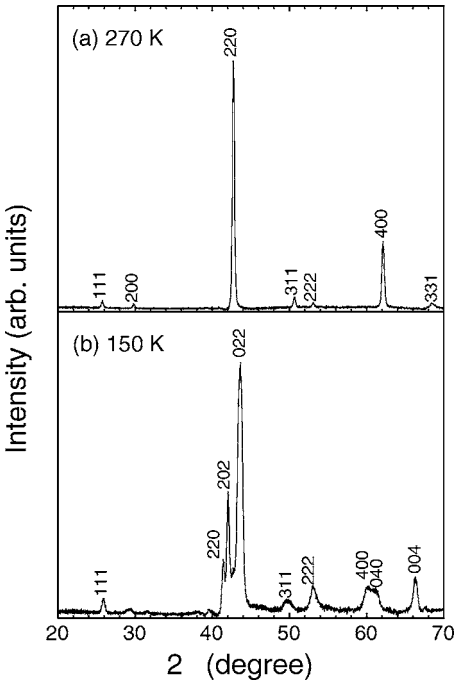

FIG. 3. X-ray diffraction patterns for $Ni_{50.3}Mn_{35.3}Sn_{14.4}$ ribbons measured at 270 K (a) and 150 K (b). The crystal structures are $L2_1$ austenite and 7M orthorhombic martensite, respectively.

martensite is different to that found in bulk materials with closer compositions such as $Ni_{50}Mn_{36}Sn_{14}$ (4O) (Refs. 4 and 5) or $Ni_{50}Mn_{37}Sn_{13}$ (10M).[2] It is worthy of mention the magnetically soft behavior of austenite that reaches a large magnetization value at 50 Oe. The transition from ferromagnetic to paramagnetic state for this phase occurs at 313 K. The structural transformation shows start and finish temperatures of $M_S=226$ K, $M_f=218$ K, $A_S=237$ K, and $A_f=244$ K, while a thermal hysteresis of 21 K between cooling and heating curves was measured. These values are close to those reported for the bulk $Ni_{50}Mn_{36}Sn_{14}$ alloy.[4,6] $M(T)$ at the FH curve slightly decreases monotonously until the transformation starts, and coincides with the magnetization value for the FC curve in the 10–215 K range. At 50 kOe, heating and cooling $M(T)$ show two well distinct ferromagnetic regions illustrating a reversible and abrupt change in magnetization as well as the field dependence of the martensitic transformation. A decrease in the characteristic temperatures of the structural transformation is observed (estimated values: $\Delta M_S=-11$ K, $\Delta M_f=-8$ K, $\Delta A_S=-7$ K, and $\Delta A_f=-7$ K). The abrupt change of $M(T)$, displayed in the inset of Fig. 2 around crystal transition temperatures, suggests that significant and positive magnetic entropy change ΔS_M associated with the inverse magnetocaloric effect could be expected. The maximum value of magnetic entropy change ΔS_M at a field of 20 kOe obtained from the magnetization isotherms (~ 5 J kg^{-1} K^{-1}) is, in fact, large and comparable to that found in bulk materials of similar composition.[7]

Hysteresis loops measured at 270 and 150 K (Fig. 4), underline the ferromagnetic ordering of austenite and martensite. When the magnetic field is applied parallel to the rolling direction, $M(H)$ curve for austenite shows high susceptibility at low fields and fast approach to saturation [Fig. 4(a)]. This magnetically soft behavior is a consequence of the low anisotropy of austenite in agreement with its cubic symmetry. Domain walls displacement would be the domi-

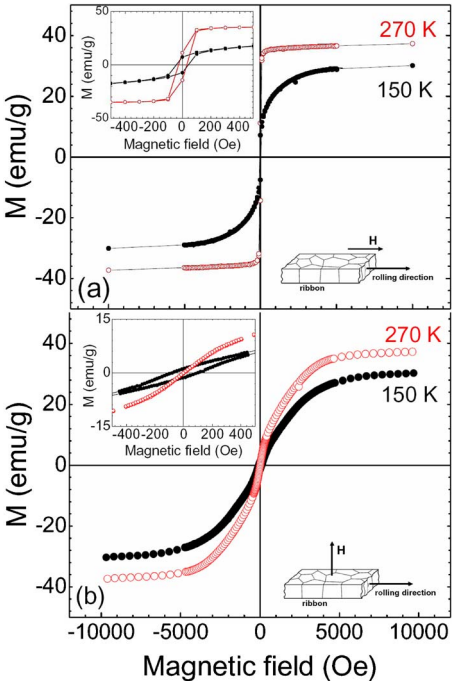

FIG. 4. (Color online) Hysteresis loops for $Ni_{50.3}Mn_{35.3}Sn_{14.4}$ ribbons measured at 150 and 270 K with the field applied parallel to the rolling direction (a), and perpendicular to the ribbon plane (b). Insets: zoom into the low field range.

nant magnetization process in this phase. Furthermore, the loop shape suggests that the easy magnetization direction lies along the rolling direction and therefore perpendicular to the major axis of columnar grains. A different situation is found for martensite, since the influence of rotation process can be observed from low fields up to 5 kOe when $M(H)$ approaches its saturation value, indicating that anisotropy axis for this phase tilts from the rolling direction. The inset of Fig. 4(a) zooms into the low magnetic field region. Coercive field H_C for austenite is 28 Oe, while H_C for martensite is 52 Oe. Hysteresis loops for both phases do not saturate up to near 10 kOe when the magnetic field is applied perpendicular to the ribbon plane [Fig. 4(b)]. The loop is anhysteretic for austenite but H_C is 88 Oe for martensite and harder magnetic properties are found (as the inset shows), confirming that magnetization easy axes are in the ribbon plane for both phases.

The effect of magnetic field on reverse transformation was studied by measuring magnetization isotherms, under increasing and decreasing the field, in the transformation temperature range. Before recording each isotherm, the sample was cooled down to 200 K (to ensure the start of measurement in martensitic state), and then heated to the measuring temperature in zero field. After temperature stabilization, the isotherm is measured and the cycle is repeated. $M(H,T)$ curves are shown in Fig. 5. All of them have the signature of metamagnetism owing to the effect of the magnetic field on the transformation. Consequently, a hysteresis between field-up and field-down curves is observed. The behavior is emphasized as the temperature approaches to 240 K, where the inflection point of the low-field $M(T)$ curve was obtained (see inset of Fig. 2). At this temperature, a well defined discontinuity in the first derivative of the field-up $M(H)$ curve is observed at $H=17.3$ kOe. Over this field, a progressive magnetic field induced transformation

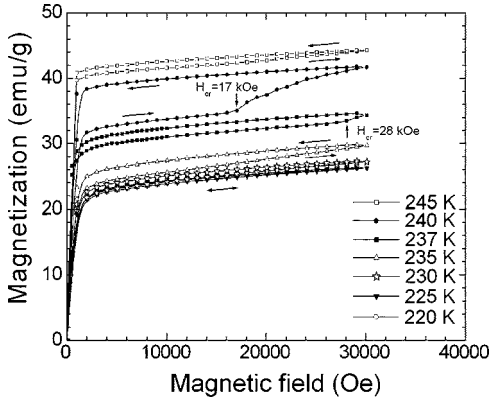

FIG. 5. Magnetization isotherms for $Ni_{50.3}Mn_{35.3}Sn_{14.4}$ ribbons measured in the temperature interval where the reverse martensitic transformation occurs. The vertical arrow indicates the critical magnetic field value at which the field-induced starts.

from martensite to austenite is observed. As temperature approaches to "pure" austenitic or martensitic phase existence regions, these effects vanish.

In summary, martensitic transformation from cubic bcc $L2_1$ to $7M$ orthorhombic structure was observed in $Ni_{50.3}Mn_{35.3}Sn_{14.4}$ melt spun ribbons exhibiting highly ordered columnar grains running through the ribbon thickness. Magnetization easy axis lies along the rolling direction for austenite while anisotropy direction for martensite tilts out of it. Around A_S, a field over 17 kOe induces a progressive reverse martensitic transformation. The large inverse magnetocaloric effect (comparable to that of bulk materials) originated from the abrupt change in magnetization around structural transition, together with advantages of the single step production by melt spinning, points to the fact that the NiMnSn Heusler ribbons could be of potential interest as magnetocaloric material.

FICYT is acknowledged by J.L. Sánchez Llamazares (Contract No. COF07-013). This work has been supported by the Spanish MEC under Projects Nos. MAT2006-13925-C02-01, MAT2006-13925-C02-02, NAN-2004-09203-C04-C03, and NAN-2004-09203-C04-C02.

[1]Y. Sutou, Y. Imano, N. Koeda, T. Omori, R. Kainuma, K. Ishida, and K. Oikawa, Appl. Phys. Lett. **85**, 4358 (2004).
[2]T. Krenke, M. Acet, E. F. Wassermann, X. Moya, L. Mañosa, and A. Planes, Phys. Rev. B **72**, 014412 (2005).
[3]X. Moya, L. Mañosa, A. Planes, T. Krenke, M. Acet, and E. F. Wassermann, Mater. Sci. Eng., A **438-440**, 911 (2006).
[4]P. J. Brown, A. P. Gandy, K. Ishida, R. Kainuma, T. Kanomata, K.-U. Neumann, K. Oikawa, B. Ouladdiaf, and K. R. A. Ziebeck, J. Phys.: Condens. Matter **18**, 2249 (2006).
[5]V. Khovaylo, V. Koledov, V. Shavrov, V. Novosad, A. Korolyov, M. Ohtsuka, O. Savel'eva, and T. Takagi, Funct. Mater. **13**, 474 (2006).
[6]K. Koyama, K. Watanabe, T. Kanomata, R. Kainuma, K. Oikawa, and K. Ishida, Appl. Phys. Lett. **88**, 132505 (2006).
[7]T. Krenke, E. Duman, M. Acet, E. F. Wassermann, X. Moya, L. Mañosa, and A. Planes, Nat. Mater. **4**, 450 (2005).
[8]X. Moya, L. Mañosa, A. Planes, T. Krenke, E. Duman, M. Acet, and E. F. Wassermann, J. Magn. Magn. Mater. **316**, e572 (2007).
[9]Z. D. Han, D. H. Wang, C. L. Zhang, H. C. Xuan, B. X. Gu, and Y. W. Du, Appl. Phys. Lett. **90**, 042507 (2007).
[10]A. Planes, L. Mañosa, X. Moya, T. Krenke, M. Acet, and E. F. Wassermann, J. Magn. Magn. Mater. **310**, 2767 (2007).
[11]K. Koyama, H. Okada, K. Watanabe, T. Kanomata, R. Kainuma, W. Ito, K. Oikawa, and K. Ishida, Appl. Phys. Lett. **89**, 182510 (2006).
[12]J. D. Santos, T. Sanchez, P. Alvarez, M. L. Sanchez, J. L. Sánchez Llamazares, B. Hernando, Ll. Escoda, J. J. Suñol, and R. Varga, J. Appl. Phys. **103** (2008).